HYDROGEN EFFECT ON FATIGUE AND FRACTURE OF PIPE STEELS

Capelle, J.[1], Gilgert, J.[1] and Pluvinage, G.[1]
[1] Laboratoire de mécanique Biomécanique Polymère Structure (LaBPS),
Ecole Nationale d'Ingénieurs de Metz (ENIM),
Ile du Saulcy, Metz, 57045, France, capelle@enim.fr

ABSTRACT

Transport by pipe is one the most usual way to carry liquid or gaseous energies from their extraction point until their final field sites. To limit explosion risk or escape, to avoid pollution problems and human risks, it is necessary to assess nocivity of defect promoting fracture. This need to know the mechanical properties of the pipes steels. Hydrogen is considered to day as a new energy vector, and its transport in one of the key problems to extension of its use. Within the European project NATURALHY, it has been proposed to transport a mixture of natural gas and hydrogen. 39 European partners have combined their efforts to assess the effects of hydrogen presence on the existing gas network. Key issues are durability of pipeline material, integrity management, safety aspects, life cycle and socio-economic assessment and end-use. The work described in this paper was performed within the NATURALHY work package on 'Durability of pipeline material'. This study makes it possible to emphasize the hydrogen effect on mechanical properties of several pipe steels as X52, X70 or X100, in fatigue and fracture, and in two different environments: air and hydrogen electrolytic.

1.0 EUROPEAN GAS NETWORK

Nowadays, pipelines for gas and oil transportation are very significant components of national as well as global economic infrastructures. Huge plans for installation of new transcontinental pipelines require increased attention regarding their reliable and safe exploitation. The European gas pipelines network plays very important role for national economies as well as global. This importance will permanently increase with prospective plans of introducing of European hydrogen energy infrastructure [1, 2] and the possible use of existing pipeline networks for transportation of natural gas and hydrogen mixtures. This idea comes from the fact that this network has a length of above 185,000km [3].

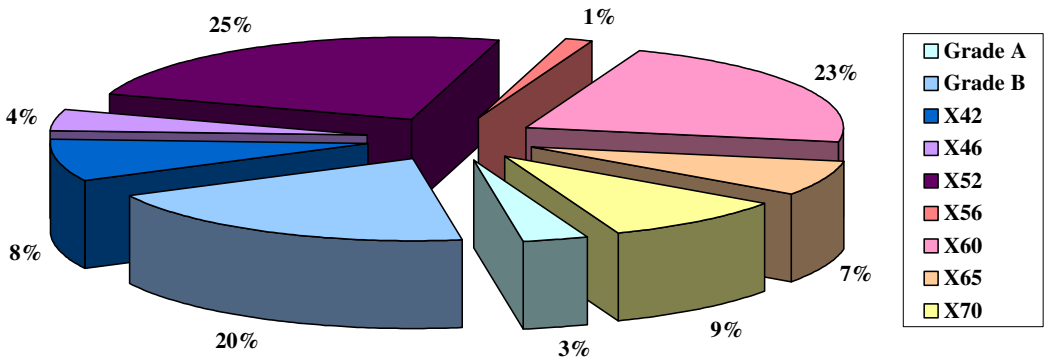

Figure 1. Distribution of different grades of steel in the European gas network in 2004 [4]

Within the European project NATURALHY [5], 39 European partners have combined their efforts to assess the effects of the presence of hydrogen on the existing gas network. Key issues are durability of pipeline material, integrity management, safety aspects, life cycle and socio-economic assessment and end-use. The work described in this paper was performed within the NATURALHY work package on 'Durability of pipeline material'. The problems of crack initiation in fatigue and fractures emanating

from stress concentrators are at origin of more than 90% of service failure. The presence of a geometrical discontinuity such as a gouge will weaken the fracture resistance of the pipe steel. It reduces the section of the pipe, while making it more sensitive to service pressure and efforts provoked by soil movements. In this paper, several fatigue and fracture tests have been performed in two environments, air and hydrogen in order to measure the hydrogen embrittlement index of pipe steels. The chosen pipe steels are X52 and, X70 representative of the used steel in the actual gas network (respectively 25% and 9%) and X100 pipe steel representative of the high strength steel used in new pipe lines with larger diameter and working at higher service pressure. (Fig. 1).

2.0 MATERIAL AND TEST CONDITIONS

2.1 Studied steels

The API 5L X52 is an ancient steel used for transmission of oil and gas during 1950-1960, the API 5L X70 has been introduced in pipe networks since 1970. The API 5L X100 studied since 1980 [6], was only very recently introduced in the natural gas network. The standard chemical composition and mechanical properties of these steels are shown in tables 1 and 2.

Table 1. Chemical composition of steels X52, X70 and X100 (in weight %).

	C	Mn	Si	Cr	Ni	Mo	S	Cu	Ti	Nb	Al
X52	0.206	1.257	0.293	0.014	0.017	0.006	0.009	0.011	0.001	<0.03	0.034
X70	0.125	1.68	0.27	0.051	0.04	0.021	0.005	0.045	0.003	0.033	0.038
X100	0.059	1.97	0.315	0.024	0.23	0.315	0.002	0.022	0.022	0.046	0.037

Table 2. Mechanical properties of steels X52, X70 and X100.

	E (GPa)	σ_Y (MPa)	σ_U (MPa)	A%	n	K (MPa)
X52	194	437	616	23.14	0.106	780.2
X70	215	590	712	18.3	0.047	757.8
X100	210	866	880	6.75	0.006	903.6

Where E, σ_Y, σ_U, $A\%$, n, and K are the Young's modulus, yield stress, ultimate strength, ultimate elongation, hardening exponent, and hardening coefficient, respectively.
The material stress strain behaviour is described by the Ludwik law according to:

$$\sigma = K\varepsilon_p^n, \quad (1)$$

2.2 Specimen used

Two specimen types have been used: standard Compact Tension (CT) specimens have been chosen to perform fracture toughness test, and the non standard Roman Tile (RT) for fatigue test.

Roman tile specimen are not precracked but exhibiting a notch to be more representative of defect produced by external interference such as contact between pipe and excavator for example.

Tests on Compact Tensile specimen (CT) had been performed, according to French standards NF A 03-180 [6] and NF A 03-182 [7]. Geometry and dimensions of specimens are given in Fig. 2.

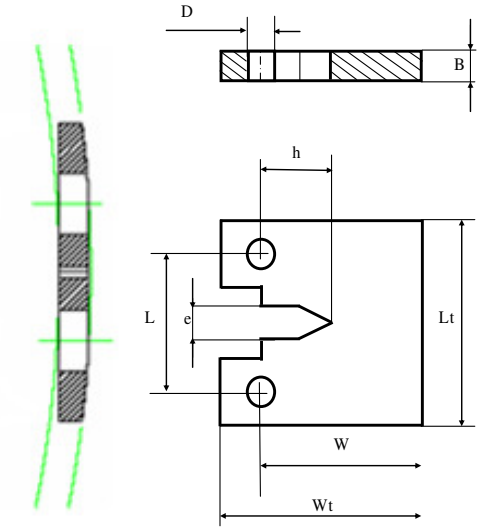

Figure 2. CT specimen (geometry and direction in the pipe wall thickness)

With L_t=120mm, L=55mm, D=20mm, B=10mm, W=100mm, W_t=125mm, e=5mm and h=46mm.

For defects assessment of scratches and gouges, it is necessary to determine notch fracture toughness in radial direction. The name “Roman Tile” specimen is relative to geometry, Fig. 3, notch is then representative of a longitudinal gouge like defect. The use of this particular geometry is explained by the impossibility due to low thickness and pipe important curvature to machining a standard three point bending specimen.

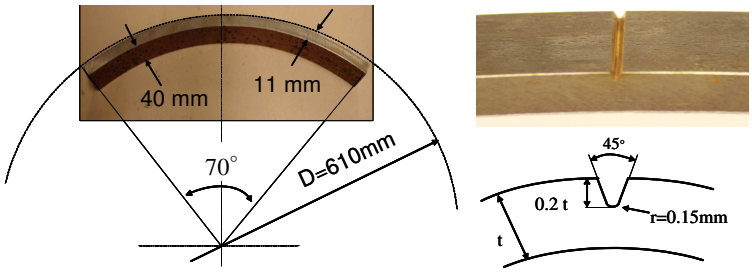

Figure3. Roman Tile specimen

The V-notch with the notch opening angle of 45° and root radius of 0.15 mm was machined to a depth of size a, aspect ratio is $a/W =$ 0.2, W corresponding to wall thickness. A special testing device has been developed for this purpose.

2.3 Electrolytic hydrogen charging

Electrolytic hydrogen charging was conducted in a special solution called NS4 with pH = 6.7, [8]. Chemical composition is given in Table 3. NS4 solution was prepared from these chemical compounds and distilled deionised water. The solution volume is about 17 litters. A pump is used to have always a homogeneous solution during the fatigue test. This solution has a natural pH between 8 and 8.5. A precise test control indicates during test an initial value pH = 8.56. To decrease the pH until 6.7 during the fatigue test, we have used a CO_2 gas bubbling and another N_2 gas one to stabilize pH solution and take off inside oxygen. During tests, pH level is controlled and monitored 6.6 and 6.7. The bubbling gas was set with the following composition: 80% of N_2 and 20% of CO_2 gas. In these conditions, i.e. in deoxygenated, near-neutral pH solution, the hydrogen atoms are generated on the steel surface by electrochemical reduction of water molecules:

$$H_2O + e \rightarrow H_{ads} + OH^-, \quad (2)$$

The adsorbed hydrogen atoms can subsequently combine into H_2 molecules by the chemical reaction:

$$2H_{ads} \rightarrow H_2, \quad (3)$$

or the electrochemical reaction:

$$H_{ads} + H_2O + e \rightarrow H_2 + OH^-, \quad (4)$$

Table 3. Chemical composition of NS4 solution (gram/litre), [11]

Chemical compound	Formula	Concentration (mg/L)
Potassium chloride	KCl	122
Sodium hydrogenocarbonate	$NaHCO_3$	483
Hydrated calcium chloride	$CaCl_2,2H_2O$	181
Hydrated magnesium sulfate	$MgSO_4,7H_2O$	131

Accounting the fact that a steady state condition of hydrogen charging cannot be imposed nor obtained in a freely corroding situation, a specific procedure is made. Specimens were hydrogen charged at constant polarisation potential E_{cath} = –1000 mV_{SCE}, which is slightly more negative than free corrosion potential E_{corr} = –800 mV_{SCE} for tested steel. Then, the specimens were immersed into the cell with special NS4 solution and exposed under constant potential of polarisation E_{cath} = const. The surface of auxiliary electrode was parallel to notch plane with the distance h = 20 mm.

2.4 testing devices

For standard specimen, used device is according to French Standard recommendations [6]. RT specimens are 3 points bending loaded and a special device was design. The specimen was loaded by three-point bending through a support A and supporting rollers B and C, Fig. 4. Support and rollers were produced from Poly Vinyl Chloride (PVC) to reduce friction. The bend-test fixture was positioned on a closed loop hydraulic testing machine with a load cell of capacity ± 10 kN.

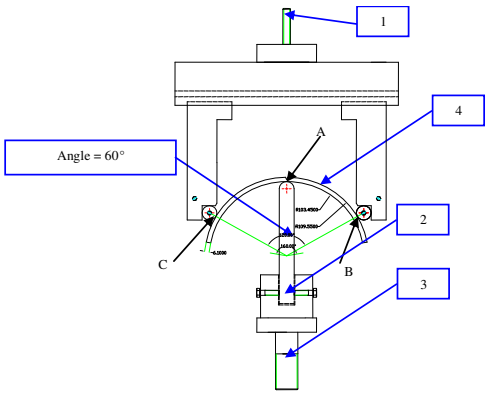

Figure 4. Roman Tile specimen fixture and assembly
1 - connection with load cell; 2 - transmitting component with rounded tip; 3 - connection with the testing machine bottom; 4 – specimen

3.0 FRACTURE TOUGNESS OF THE STUDIED PIPE STEELS

3.1 Determination of critical stress intensity factor

The studied steels do not exhibit brittle fracture and determination of critical stress intensity factor K_{Ic} is not valid according strictly to standard. However, fracture test allows to get stress intensity factor at fracture initiation, K_{Ii} .Crack initiation is detected by acoustic emission (AE), the applied load at the fist burst of acoustic energy is considered as critical load (see fig 3) . Tests are then performed with a pre crack along pipe longitudinal direction.

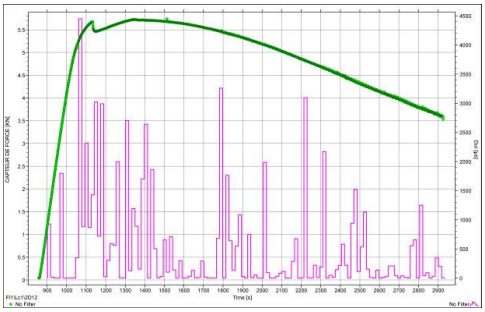

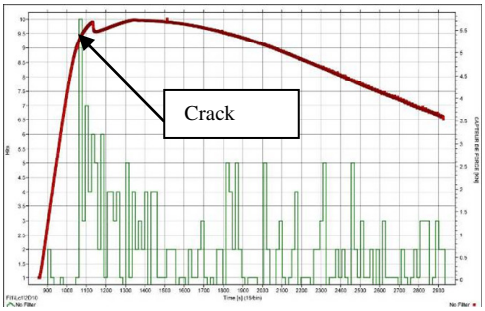

Figures 3 and 4. Curves showing Hits vs. Time (left), Duration of the acoustic emission vs. Time (right) and Load vs. Time (both)

Comparison in figures 3 and 4, between load versus time and acoustic emission versus time indicate clearly that crack initiation is close to “pop-in”. For this event, acoustic salves with the highest duration and the most important number of acoustic hits are easily detectable.
Fatigue precracking is done realised under the following experimental conditions, for all specimens:

- Wave shape: sine
- Frequency: 15Hz
- Maximum load: 7500N
- Load ratio: 0.1
- Final crack length: 9mm

During fracture test, a clip gauge is used to follow the notch opening displacement. Notch opening displacement is measured at distance z of front face of specimens,(z is the clip gauge holders thickness) Tests are carried out with a displacement rate of 0.02mm/s. From displacement at initiation v and its plastic component v_p , we get crack-tip opening displacement δ_i and, stress intensity factor at initiation K_{Ii} according to French standards [6, 7] with the following formulas:

$$\delta_i = \frac{K_{Ii}^2\left(1-\upsilon^2\right)}{2R_{p0,2}} + \frac{0{,}4\left(W-a_0\right)}{\left(0{,}4W+0{,}6a_0+z\right)}v_p\,, \tag{5}$$

$$K_{Ii} = \frac{F_i}{BW^{1/2}} f_{(a_0/W)}\,, \tag{6}$$

Values is the mean of two tests for each series (reference test in air and Test with after hydrogen electrolytic charging)

3.2 Critical notch stress intensity factor

The concept of the critical notch stress intensity factor and corresponding local fracture criterion assume that the fracture process requires a certain fracture process volume [9]. This local fracture

approach is called the Volumetric Method (VM). The fracture process volume is assumed as a cylinder with a diameter called the effective distance X_{ef}. Determination of the effective distance is based on the bi-logarithmic elastic-plastic stress distribution ahead of the notch tip. The fracture process zone is considered as the highest stressed zone with limit characterized by an inflexion point on stress distribution ie limit of zones II and zone III on in Fig. 4. This inflexion point is related to the minimum of the relative stress gradient χ which can be written as:

$$\chi(r) = \frac{1}{\sigma_{yy}(r)} \frac{\partial \sigma_{yy}(r)}{\partial r}, \tag{7}$$

The effective stress σ_{ef} of the fracture criterion is the mean stress over the distance X_{ef} of the notch tip stress distribution.

$$\sigma_{ef} = \frac{1}{X_{eff}} \int_0^{X_{ef}} \sigma_{yy}(r) \Phi(r) dr, \tag{8}$$

Here, $\sigma_{yy}(r)$ and $\Phi(r)$ are opening stress and weight function, respectively. This stress distribution is corrected by a weight function in order to take into account the distance from notch tip of the acting point and the stress gradient at this point. The notch stress intensity factor is defined as a function of the effective distance and the effective stress [8]:

$$K_\rho = \sigma_{ef} \sqrt{2\pi X_{ef}}, \tag{9}$$

and describes the stress distribution in zone III according to the following equation:

$$\sigma_{yy} = \frac{K_\rho}{(2\pi r)^\alpha}, \tag{10}$$

where K_ρ is notch intensity factor, α is the exponent of the power function of stress distribution, t. Failure occurs when notch stress intensity factor K_ρ reaches the critical value, i.e. notch fracture toughness $K_{\rho,c}$ which reflects the resistance to fracture initiation from notch tip. Determination of notch fracture toughness needs both computing of stress distribution ahead of the notch tip and along ligament by Finite Element and experimental determination of critical load defined by AE technique. This is then made through determination of effective distance and effective stress at critical load and minimum of relative stress gradient as described in Fig. 5.

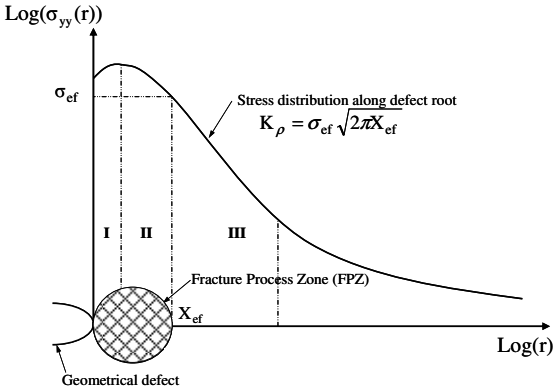

Figure 4. Schematic distribution of elastic-plastic stress ahead of the notch tip on the line of notch extension and description of the notch stress intensity factor concept.

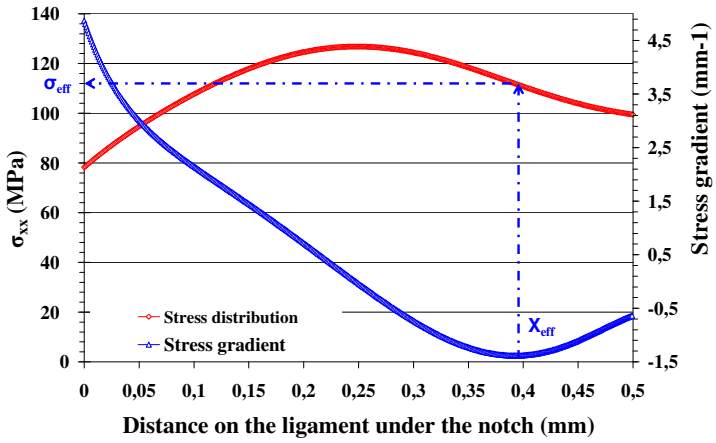

Figure5. Determination of effective distance using the relative stress gradient method

Notch fracture toughness depends on notch radius and more precisely notch critical stress intensity factor is proportional to the square root of the notch radius above below a critical notch radius value ρ_{cr} [9].

$$K_{\rho,c} = \therefore \sqrt{\rho} \quad for \ \rho \geq \rho_{cr}, \tag{11}$$

$$K_{\rho,c} = K_{Ic} \ for \ \rho < \rho_{cr}, \tag{12}$$

One notes that fracture toughness measured on specimen with a notch radius greater than ρ_{cr} is denoted $K_{\rho,c}$. This increase of fracture toughness with notch radius is due to the increase of notch plastic zone and consequently the total work of fracture. The critical notch radius corresponds to the fact that the notch plastic zone volume is equal to the fracture process zone volume [11].The dependence of notch fracture toughness makes necessary to measure the notch fracture toughness with the corresponding gouge radius. In the following, the notch radius ρ = 0.15mm is considered as representative of a severe defect and chosen for conservative reasons. This value compared with other obtained from low strength steels, is probably below the critical notch radius value.

4.0 FATIGUE TEST CONDITIONS

The test set-up of three-point bending test for “roman tile” specimens and testing machine are described in Fig. 6. The bend-test fixture is similar than those used for static test and. The bend-test fixture is positioned on the closed loop hydraulic testing machine with load cell capacity ±10 kN.

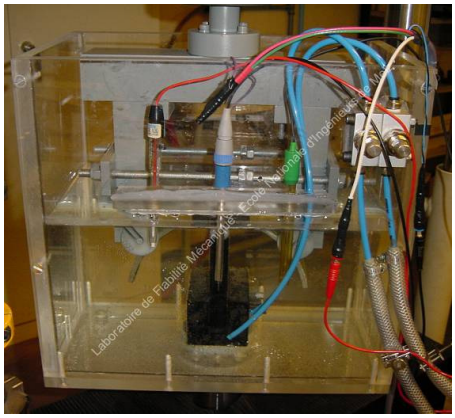

Figure 6. Devices used for notch fracture toughness tests under hydrogen presence

Applied load, frequency and fatigue wave shape (sine) cycle (sinusoidal) were monitored on machine the control panel. Hydrogen charging was made using the same cell filled with NS4 solution used for fracture tests. Tests conditions are given in table 4.

Table 4. Fatigue test conditions

Wave shape	Sine
Frequency :	0.05 Hz
Load ratio	0.5 (in service condition 0.57)
Working potential	- 1 V_{sce}
Electrolytic solution	Natural Soil 4 (NS4)
Solution pH	Regulated between 6.66 and 6.74

Crack initiation was also detected by acoustic emission and Wöhler curves were drawn at both initiation and failure. A classical power fit is in accordance with Basquin's law has been made:

$$\Delta\sigma = \sigma^{'} f\left(N_R\right)^b, \tag{13}$$

where $\sigma_f^{'}$ is the fatigue resistance and b the Basquin's exponent.

5.0 RESULTS

5.1 Fracture toughness

Fracture toughness expressed in term of $K_{\rho,i}$ is determined over 8 tests in air and over two tests when electrolytic hydrogen charging is done. . Results are given in table 5 for tests in air, and table 6 for tests with electrolytic hydrogen charging.

Table 5. X 52 $K_{\rho,i}$, tests in air.

Test n°	1	2	3	4	5	6	7	8
Critical load (N)	9300	8300	9350	9180	8710	9350	10120	8850
$K_{\rho,i}$ (MPa√m)	69,77	62,99	70,53	69,08	65,45	70,53	79,12	66,51
Mean critical load (N)				9145				
Mean $K_{\rho,i}$ (MPa√m)				69,25				
Standard deviation (MPa√m)				4,81				

Table 6. X 52 $K_{\rho,i}$ with electrolytic hydrogen charging

Holding time Time of loading	7 days		11 days		20 days	
Test #	1	2	3	4	5	6
Critical load (N)	8100	9340	8810	8500	8900	8790
$K_{\rho,i}$ (MPa√m)	61,41	70,53	65,94	64,03	66,51	65,94
Mean critical load (N)				8740		
Mean Kρ,i (MPa√m)				65,73		
Standard deviation (N)				3,01		

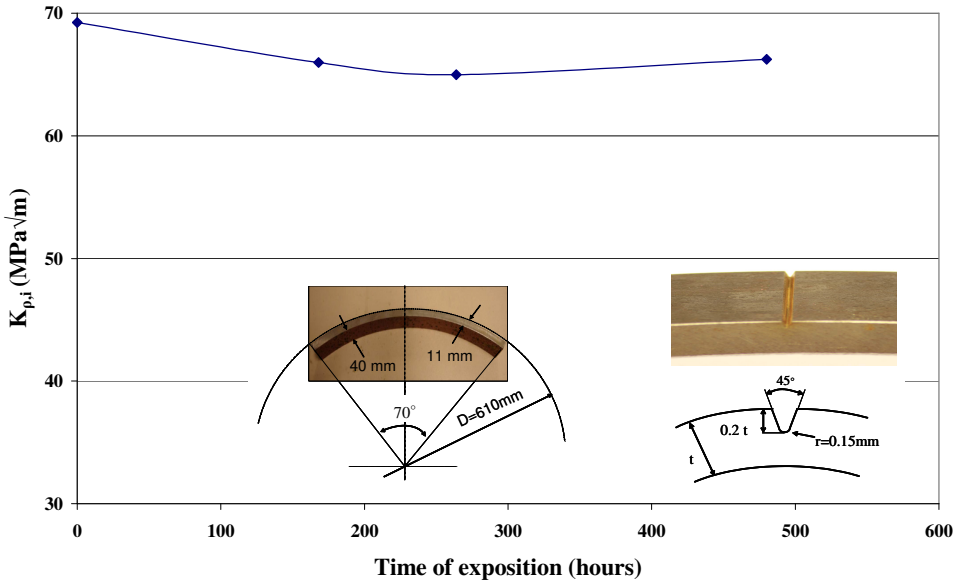

Figure7. Fracture toughness of API 5L X52 steel $K_{\rho,c}$ vs. holding time of electrolytic hydrogen charging

Influence of holding time of electrolytic hydrogen charging has been studied only on API 5L X52 steel and can be seen on figure 7. One note that hydrogen embrittlement is small. After 480 hours under electrolytic hydrogen charging, fracture toughness decreases only by 5%.

In the following, fracture toughness K_{Ii} of the three steels (X52, X70 and X100) is determined on CT pre cracked specimens, and for constant electrolytic hydrogen charging holding time of 15 days. All results are presented in table 7.

Table 7. K_{Ii} in hydrogen environment for X 52, X70 and X100 steels

		$K_{I,i}$ (MPa√m)	$K_{I,i\ mean}$ (MPa√m)	H_2 effect (%)	δ_i (mm)	$\delta_{i\ mean}$ (mm)	H_2 effect (%)
API 5L X52	AIR CT1	97,59	95,54	10,46	0,215	0,178	44,70
	AIR CT2	93,49			0,142		
	H_2 CT1	85,55	85,55		0,098	0,098	
	H_2 CT2	-----			----		
API 5L X70	AIR CT1	117,99	118,59	4,74	0,102	0,112	19,90
	AIR CT6	119,19			0,123		
	H_2 CT2	111,10	112,97		0,096	0,090	
	H_2 CT5	114,84			0,083		
API 5L X100	AIR CT1	159,98	151,82	0,80	0,125	0,108	-11,60
	AIR CT5	143,66			0,091		
	H_2 CT2	155,85	150,61		0,094	0,121	
	H_2 CT3	145,37			0,147		

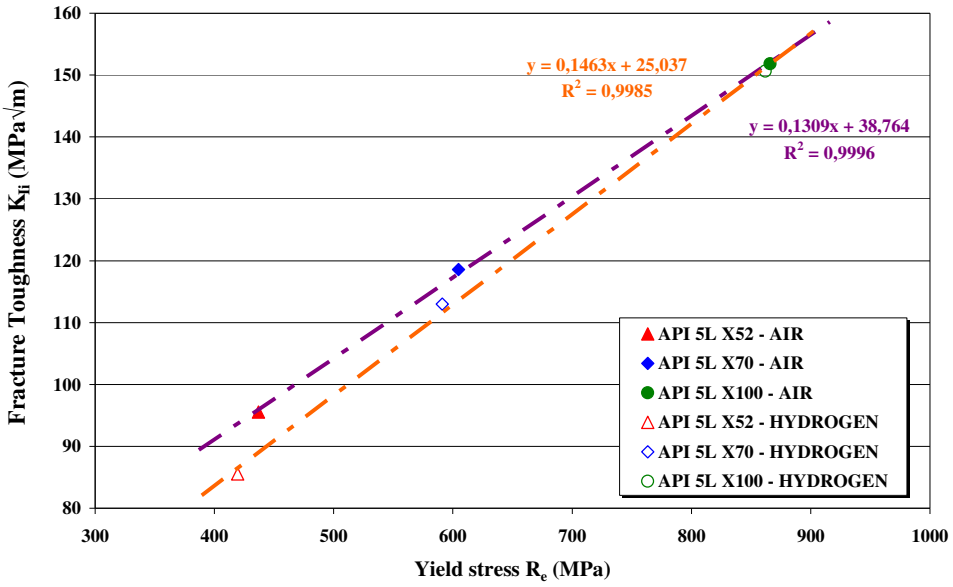

Figure 8. Fracture toughness of the three steels K_{Ii} vs. Yield stress in air and hydrogen environment

Mean value of fracture toughness is plotted versus yield stress for the three steels and for the two environment in figure 8. One note that yield stress and fracture toughness are close for the two environments and X100 is practically non sensitive to hydrogen embrittlement. One remarks that fracture toughness increases with yield stress which is not consistent with a simple local fracture criterion such as RKR criterion for which fracture toughness decreases when yield stress increases. Explanation is probably done by steel quality which has been strongly improved since the 60's when X52 was produced. It is important to underline that critical crack opening displacement (CTOD) is more sensitive to influence of yield stress and hydrogen embrittlement and seems to be a preferable fracture criterion for pipe material selection.

5.2 Wöhler curves of API X52 under air and electrolytic hydrogen charging.

Only tests on steel API 5L X52 have been realized. Wöhler curves are plotted from fracture data (standard representation) and initiation data (detected by acoustic emission). Results are presented in table 8.

Table 8. X 52 fatigue endurance parameters with and without hydrogen charging

	Air At initiation	Air At failure	H_2 At initiation	H_2 At failure
Fatigue resistance	321 MPa	336MPa	296 MPa	301 MPa
Basquin's exponent	-0,017	- 0,020	-0,011	-0,012

We note an important decrease of life duration after electrolytic hydrogen charging, (about 70%) Fig. 7. Electrolytic hydrogen charging affects particularly time to initiation 60% of life duration is used for to crack initiation in air but 80% with hydrogen influence.

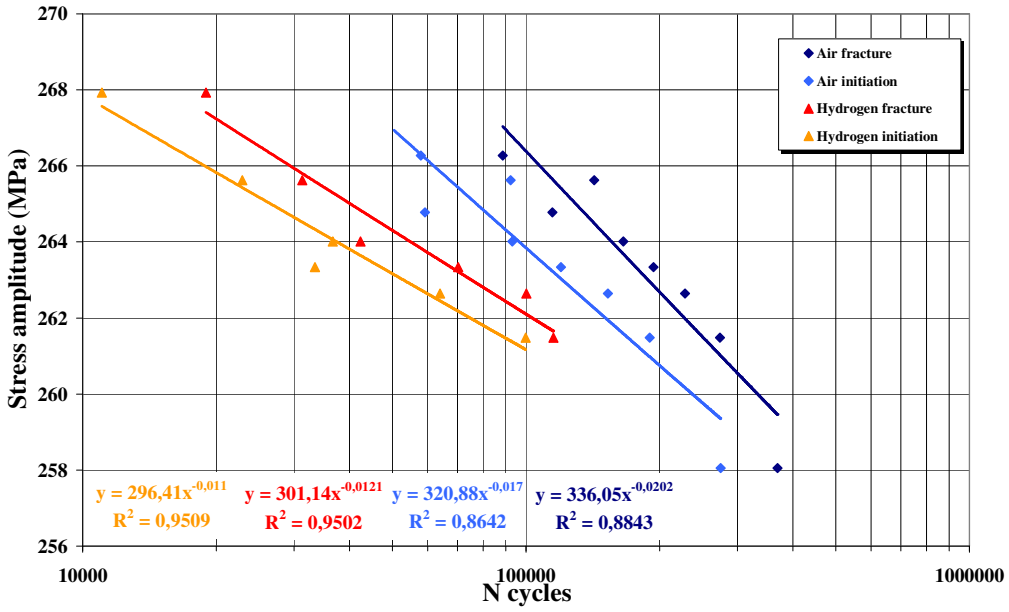

Figure 9. Fatigue endurance curves at initiation and at failure of API X52 steel with and without hydrogen charging.

6.0 CONCLUSION

Hydrogen effect on fracture is very low, for three steels studied here. But first results on fatigue show that life duration can be decreased by 70%, for the oldest steel. One important point is the impact of hydrogen on the time of crack initiation, hydrogen promote crack propagation. So it is very important to find procedure to detect crack on pipe, to be anticipate pipe burst.

REFERENCES

1. Fernandes T. R. C., da Graça Carvalho F. C. and M., "HySociety" in support of European hydrogen projects and EC policy. International Journal of Hydrogen Energy, 30, pp 239-245, (2005)
2. Mulder G., Hetland J. and Lenaers G. Towards a sustainable hydrogen economy: Hydrogen pathways and infrastructure. International Journal of Hydrogen Energy, 32, Issues 10-11, pp 1324-1331, (2007)
3. Association Suisse de l'Industrie Gazière (ASIG), site Internet : www.gaz-naturel.ch, (2004)
4. 6th Report of the European Gas Pipeline Incident Data Group, 1970-2004, (2005)
5. NaturalHy Project, *http://www.naturalhy.net*
6. NF A 03-180, "Détermination du facteur d'intensité de contrainte critique des aciers", Afnor, (1981)
7. NF A 03-182, "Détermination de l'écartement à fond de fissure (CTOD)", Afnor, (1987)
8. J. Capelle, I. Dmytrakh, G. Pluvinage, "Electrochemical Hydrogen Absorption of API X52 Steel and its Effect on Local Fracture Emanating from Notches", Structural Integrity and Life, volume 9, n° 1, pp. 3–8, (2009)
9. G Pluvinage "Fracture and Fatigue emanating from stress concentrators"; Kluwer, (2003).
10. Akourri O, Louah M, Kifani A, Gilgert G, Pluvinage G., "The effect of notch radius on fracture toughness J_{IC} ", Eng Fract Mech 65, pp 491-505, (2000)

11. J. Capelle, J. Gilgert, I. Dmytrakh, G. Pluvinage, “Sensitivity of pipelines with steel API X52 to hydrogen embrittlement”, International Journal of Hydrogen Energy 33, issue 24, pp 7630-7641, (2008)